WORLD CONFERENCE ON TIMBER ENGINEERING 2025
BRISBANE, AUSTRALIA
Advancing Timber for the Future Built Environment

MECHANICAL PROPERTIES AND FAILURE CRITERIA OF WOOD UNDER COMBINED NORMAL-SHEAR LOADING

Li-Peng Zhang[1], Reza Andasht Kazeroon [2]

ABSTRACT: In this study, combined normal-shear behaviors of six type of specimens were conducted. An auxiliary device was designed and equipped to testing machine to help achieving combined normal-shear loading. Failure modes, and shear stress-strain curves under different normal stresses were obtained. The applicability of several commonly used orthotropic strength criteria including Hill, Tsai-Hill, Tsai-Wu, Hoffman, et al. to predict the combined tension/compression and longitudinal shear failure were systematically assessed according to test data from the experiment as well as existing literature. Results indicated that normal stress greatly affects the shear failure mode and performance. The best applicable normal stress ranges of the examined failure criteria were confirmed.

KEYWORDS: wood, combined normal-shear behavior, experiment, failure mode, strength criteria

[1] Li-Peng Zhang, School of Civil Engineering, Xi'an Universisty of Architecture and Technology (XAUAT), Xi'an, China, lpgzhang@xauat.edu.cn

[2] Reza Andasht Kazeroon, School of Civil Engineering, Xi'an Universisty of Architecture and Technology (XAUAT), Xi'an, China, reza.andasht @xauat.edu.cn

https://doi.org/10.52202/080513-0018

1 – INTRODUCTION

Wood has porous and inhomogeneous microstructure and is considered an approximately cylindrical anisotropic material due to its growth ring features. By ignoring the growth ring curvature and referring to composite material mechanics, the general stress states of wood element can be represented with regard to the principal material axes of longitudinal (L), radial (R), and tangential (T), see Figure 1a. The planes normal to the L, R, and T directions are called R-T plane, L-T plane, and L-R plane, respectively. On such basis, wood mechanical problems are usually addressed on the 9-D stress space, see Figure 1b.

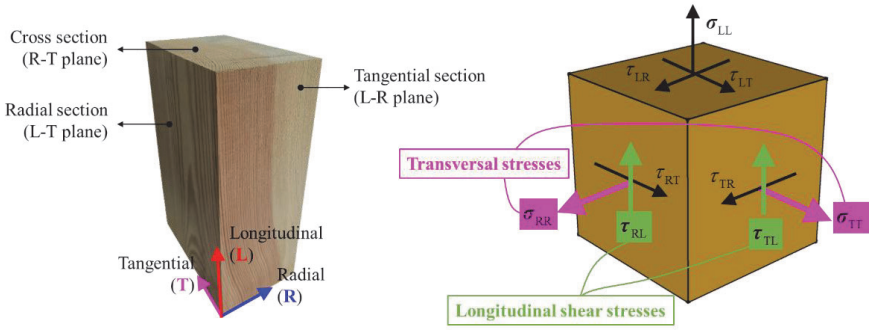

Figure 1. Principal material axes, planes, and stress element of wood.

During the past several decades, extensive research has been conducted in response to the anisotropic and nonlinear features of wood mechanical performance. Failure modes, stress-strain curves, full elastic constants, and the tensile/compressive strengths along the material axes and shear strengths in different planes for a wide range of commonly used wood species have been determined. The influence of wood structure characteristics parameters (e.g. growth ring width and latewood percentage), physical factors (e.g. density, moisture content, and temperature), sample sizes as well as loading strain rates on its mechanical coefficients have also been systematically reported. It brings designers and engineers significant and comprehensive insights into wood mechanical properties. However, the focus of the aforementioned investigations was primarily on simple stress states with merely one involved stress component.

In practical timber structures, wood is usually subjected to more than one stress component, e.g. multiaxial stresses and combined normal-shear stresses as opposed to pure tension, compression, or shear stress [1-3]. Thus, it is significant to investigate the mechanical performance of wood under such complicated stress states, especially the latter case due to the relatively lower shear strengths.

This work focuses on the mechanical performance and predictive criterion of larch wood, a commonly used species in Chinese traditional timber structures, under combined normal and longitudinal shear stresses. Both longitudinal shear stress in the thrss orthogonal planes were considered. V-notched specimens with curved tips were specially designed. Experiments were conducted based on a uniaxial testing machine, which is responsible for shear loading; constant normal stress is obtained through lateral loading using a self-developed lever device. DIC device was used to record the whole deformation process. The influence of different normal stress levels on the shear failure modes, deformation properties, and shear strengths were evaluated. Further, the applicability of several commonly used failure criteria to different combined normal and longitudinal shear strengths was assessed.

2 – MATERIALS AND METHODS

2.1 MATERIAL

The combined perpendicular-to-grain tension/compression and rolling shear performance was experimentally investigated by Aker et al. [5] on a European wood species, Norway spruce. For comparison, a commonly utilized Asian wood species, larch grown in northeast China (*Larix gmelinii (Rupr.) Kuzen.*) and frequently used in traditional Chinese timber structures, was selected. The annual ring width (ARW) was. Additionally, the moisture content and density were determined as 11.2% and 405 kg/m3, respectively, according to GB/T 1927.4-2021 and GB/T 1927.5-2021.

2.2 SPECIMENS

As there were no existing testing methods available for the combined normal-shear performance for wood, a specially designed modified V-notched specimens with a curved tip was developed by referring to Bilko et al. [4]. This design took into consideration the importance and challenge of ensuring a pure shear stress state. The configuration and dimension of the specimens are depicted in Figure 2.Wherein, for RT specimens, “RT” means that the axial stress is applied in the radial direction and the shear stress applied in the tangential direction, same for TR specimens. The curved tips, with a radius of r =10 mm, were incorporated to generate both a pure stress state in the interested area (cross-section area: 20 mm × 28 mm) and enable appropriate normal displacement. Finite element simulation results conducted by the authors confirmed the achievement of a pure shear stress state.

https://doi.org/10.52202/080513-0018

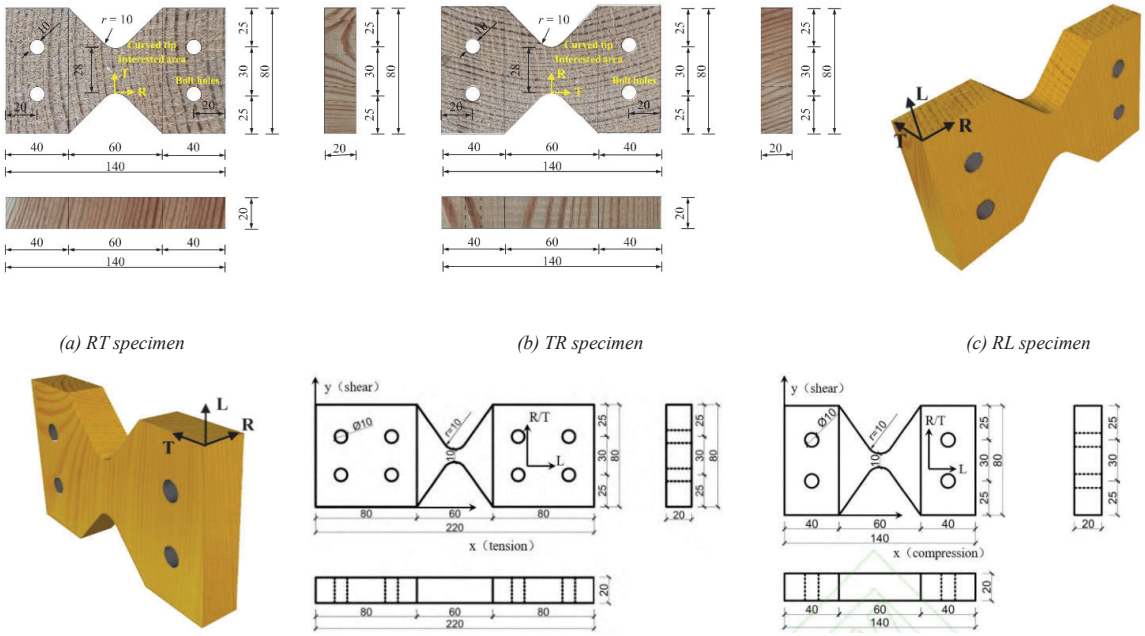

(a) RT specimen *(b) TR specimen* *(c) RL specimen*

(d) RT specimen *(e) LR/LT tension specimen* *(f) LR/LT compression specimen*

Figure 2. Configuration and dimensions of wood specimens (units: in mm).

A total of forty-eight specimens, twenty-four for each type, were prepared using a wood carving machine (brand Sign-45-200M) instead of by a carpenter. This approach aimed to minimize processing errors. Care was taken to meticulously prepare all specimens, ensuring the absence of defects such as knots, decay, or grain distortions, particularly in the areas of interest, to meet the requirement for small clear wood specimens. These specimens were utilized for both single and combined normal-shear stress interaction scenarios. The latter involved different loading conditions based on normal stress levels, including uniaxial tension, compression, shear, combined tension-shear and compression shear.

https://doi.org/10.52202/080513-0018

Table 1: Grouping of specimens

Specimen types	Number of specimens					
	LR-specimen	LT-specimen	RT-specimen	TR-specimen	RL-specimen	TL-specimen
Uniaxial tension	3	3	3	3	3	3
Uniaxial compression	3	3	3	3	3	3
Shear	3	3	3	3	3	3
Combined tension-shear	12	12	6	6	6	6
Combined compression-shear	9	9	6	6	6	6

2.3 TESTING SET-UP

A servo-hydraulic materials-testing (MTS) equipment, with loading capacity of 250 kN, was utilized in combination with a self-developed loading system to conducted the combined normal-shear tests, as illustrated in Figure 3. Since the range of the actuator far exceeds the bearing capacity of wood specimen, large error can be caused if force control loading mode is used. Therefore, displacement control mode is adopted for test accuracy. The complete loading apparatus comprises three components: the bottom frame, loading device and lever device. Normal loads were applied vertically by the testing machine, while shear loads were applied horizontally by the lever device.

The loading system serves as the central component for implementing the combined normal-shear loading function, securely affixed to the top plate of the bottom frame using bolts. Specially, two supporting baffles, combined with expanded steel plate, were welded to the bottom plate to provide stability for the self-balancing device. Four circular cross-section plain rods, each with a diameter of 39 mm, were threaded at both ends and secured to the two supporting baffles using sixteen nuts. Another steel plate, referred to as the middle sliding plate, was linked by the four rods and equipped with two sets of ball guide rails and slider combinations (BGRSC) at the bottom end, facilitating smooth horizontal movement. The friction of the loading system mainly comes from the horizontal and vertical BGRSCs during the slider moving along the ball guide rail. Before experiment, the friction was measured to be 12.5 N and 30 N, respectively, through loading without specimens. A high strength bolt was embedded in the left half part of the middle sliding plate to connect to the horizontal load sensor. The right end of the middle sliding plate was hinged with the left end of the horizontal actuating rod via a pin. It is noteworthy that the middle sliding plate conducts a critical role in horizontally transferring the normal loads without causing damage to the high strength bolt and the horizontal load sensor. With the sliding plate in place, the horizontal center alignment of the L-shaped plates, specimen, horizontal load sensor, and high strength bolt can be maintained.

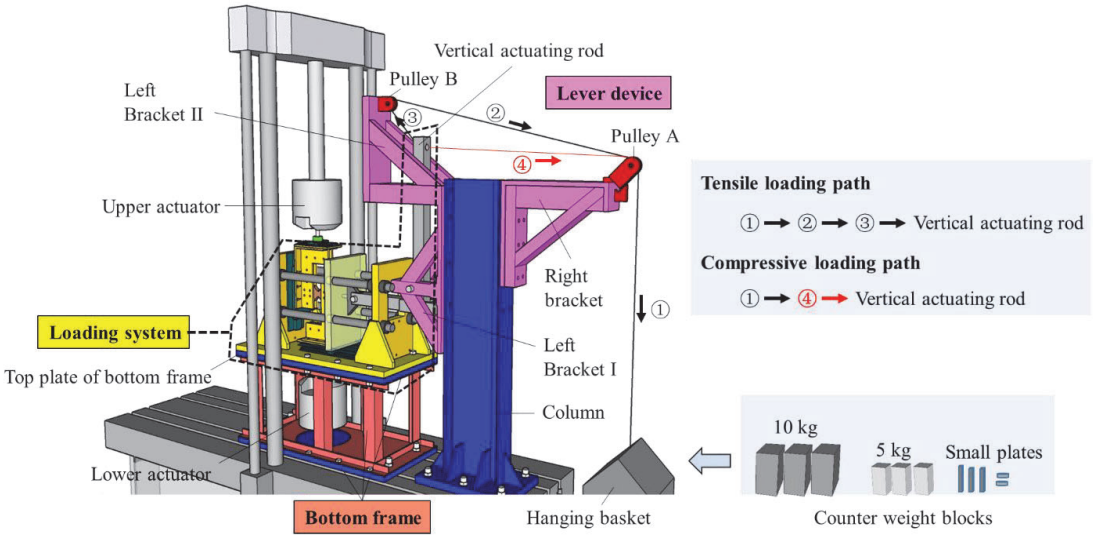

(b) 3D schematic

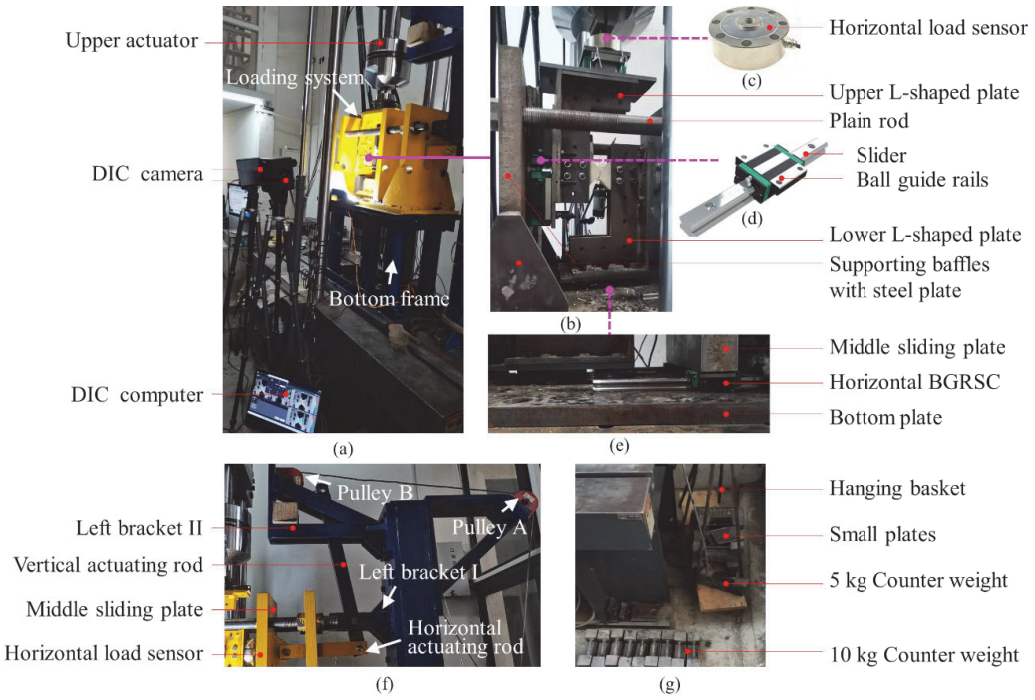

(b) Testing site

Figure 4 Pictures of the test set-up.

The pair of L-shaped steel plates mentioned above were positioned between the left supporting baffles and the middle sliding plate, facilitating the attainment of a pure shear stress state in the specimens. The upper L-shaped plate could freely slide along the vertical set of BGRSC, while the right end of the lower L-shaped plate was linked to the horizontal load sensor. Both the top surface of the upper L-shaped plate and the bottom surface of the lower L-shaped plate were outfitted with a horizontal set of BGRSC, ensuring that the vertical loading line passed through the central section of the specimen by adjusting the positions of the slide blocks. A vertical load sensor was positioned at the top end of the slide block, with a rod connected to the sensor for clamping by the testing machine. It is important to note that the loading device possesses sufficient stiffness to ensure a stabile loading process.

2.4 LOADING SCHEME AND MEASUREMENT

Uniaxial tension and compression tests involves a load-controlled process conducted by the lever device, while the shear force is performed by the MTS testing machine at a loading rate of 0.8 mm/min. The combined normal-shear tests employed a mixed loading mechanism involving both load and displacement, as illustrated in Figure 5. In this mechanism, normal stress was acquired using the lever device, similar to the uniaxial tensile and compressive cases. Subsequently, shear loading was carried out using a displacement-controlled method once the normal stress levels, $\alpha f_{t,I}$ and $\beta f_{c,I}$ were reached. To ensure sufficient loading time for the normal loading, a 2-minute free time period was allocated before the initiation of shear loading, denoted as =2.0 min.

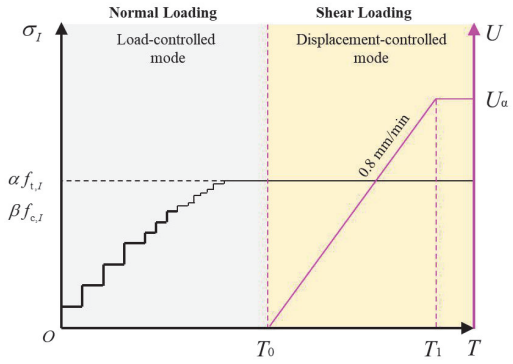

Figure 5. Combined normal-shear loading scheme.

Normal and shear forces are recoded by the equipped horizontal and vertical load sensors, respectively. DIC system including two cameras and a computer was set up to capture the full displacement and strain fields on the designated surface of the test specimens.

Initially, the specimens were coated with a thin layer of white matte paint, followed by an immediate application of black matte paint after air drying. The two Charge Coupled Device (CCD) cameras were positioned to capture images at a rate of 4 Hz, equivalent to four pictures per second. After the preparation of DIC system,

https://doi.org/10.52202/080513-0018

the calibration was conducted using a special calibration board with sizes 37mm × 52 mm. Since the values of normal strain and shear strain of a certain point on the specimen surface can be automatically calculated and output by the DIC software, thus the average values of normal and shear strains of the points on the centerline of the interested cross-section surface can be easily analyzed. Normal and shear stresses are calculated by the ratios of normal and shear forces to the area of the center cross-section, 20 mm × 28 mm, of the specimens, respectively.

3 – SHEAR STRENGTH UNDER DIFFERENT NORMAL STRESSES

The combined normal-shear strength behavior of RT and TR specimens is illustrated in Figure 6a. Where, the peak shear strength was shown under different normal stresses. It's noteworthy that while the shear strengths of TR and RT specimens under different normal stress levels show a consistent overall variation pattern, the strength data of the former exhibits greater than that of the latter. Under combined normal-shear loading, compressive stress tends to increase the shear strength of both types of specimens, whereas tensile stress generally leads to a decrease in shear strength, except for a few points attributed to material variability. Within the compressive stress range of 1.5 MPa to 7.5 MPa, the shear strength increased by approximately 48% from the average shear strength.

Figure 6b shows the combined normal-shear strengths of RL and TL specimens. It can be seen that normal stress has a significant impact on the shear strength of wood in different shear planes. The variation characteristics of shear strength of RL and TL specimens with normal stress are similar. It means that the influence of microstructure on the macroscopic interaction of normal-shear strength can be approximately ignored. Tensile stress and larger compressive stress (close to the compressive strength) have adverse effects on the shear strength for all the tested specimens. Within a certain range of compressive stresses (L.E. average compressive strength), the shear strength increases continuously. In addition, the detailed range of compressive stress is similar for RL and TL specimens. The shear strength improvement degree of RL specimens is slightly higher than that of TL specimens.

Seen from Figure 6c, the effect of tensile stress on the shear strength of LR and LT specimens is basically the same. As the tensile stress increases, the shear strength decreases continuously. When the tensile stress increases to 0.8ft, the shear strength of the specimen decreases significantly at R, by about 50%. The difference in the influence of tensile stress on the shear stiffness between the two is significant. The shear stiffness of LR specimens is basically not affected by changes in tensile stress, while the shear stiffness of LT specimens increases continuously with the increase of tensile stress.

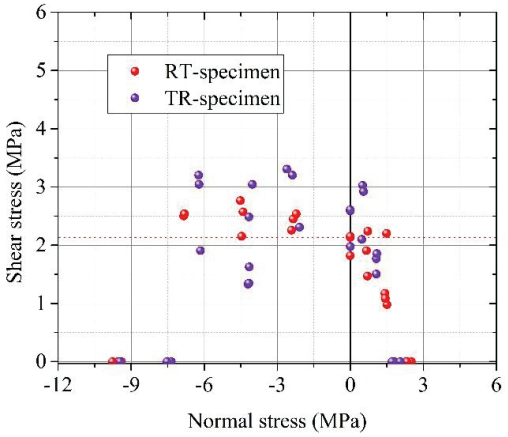

(a) RT & TR specimens

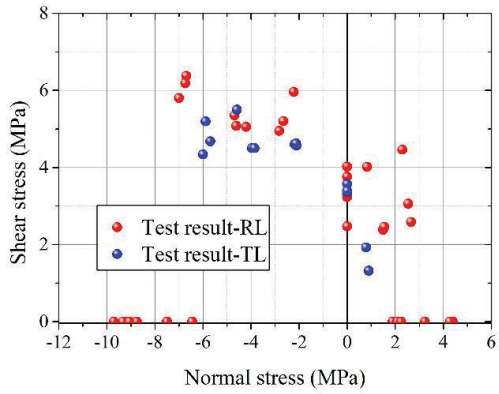

(b) RL & TL specimens

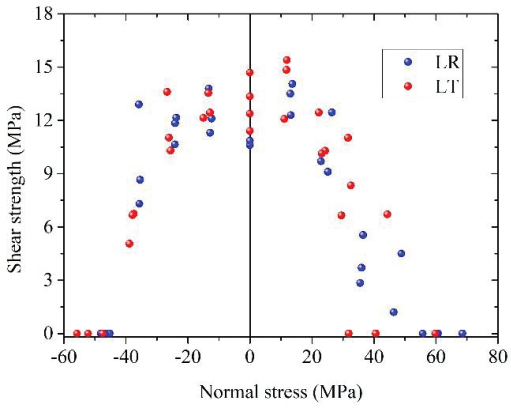

(c) LR & LT specimens

Figure 6. Combined normal-shear strength behavior of different specimens.

https://doi.org/10.52202/080513-0018

4 – APPLICABILITY OF COMMONLY USED CRITERIA

In this section, commonly used failure criteria for wood including the maximum stress, Hill, Tsai-Hill, Tsai-Wu, Hoffman, van der Put, Norris, and Hasebe criteria, et al. were assessed using normal-shear compressive testing data from this study and literature.

4.1 RT AND TR SPECIMENS

The results showed that van der Put and SIA strength criteria can better characterize the normal shear coupling strength behavior of wood in the sense of average strength, see Figure 7. However, due to the high discreteness of strength data, if the average values of uniaxial compressive strength, uniaxial tensile strength, and shear strength are substituted into the strength criteria and used for structural analysis, it will lead to significant errors in the analysis results. Therefore, the author further clarifies the uniaxial compressive strength, uniaxial tensile strength, and shear strength coefficient of error （± 40%） that need to be considered in structural analysis, which can be used as a reference in structural analysis. Van der Put-η （η=1.0, 0.6, 1.4) represent that the average tensile and shear strengths were magnified or reduced by η times and then submitted to the van der Put equation to fitting the combined normal-shear strength data; the same situation for SIA-265 criterion.

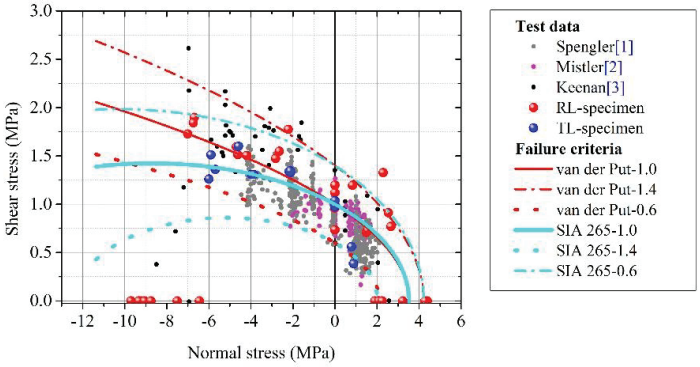

(a) Hill, Hasebe type, Mistler and Maximum stress criteria

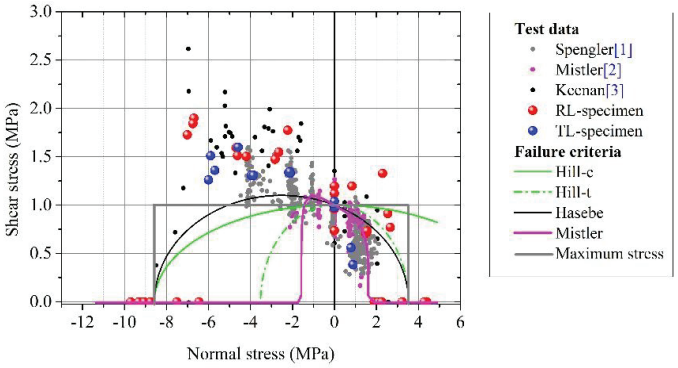

(b) van der Put and SIA 265 criteria

Figure 7. Comparison of commonly used criteria for wood with combined transverse tension/compression and longitudinal shear strength data.

4.2 RL AND TL SPECIMENS

Based on the normalized test data of this article and Aker et al. [4], the comparison of these orthotropic strength criteria is illustrated in Figure 8. Wherein, “DR-specimen” and “DT-specimen” in Aker et al. [4] corresponds to the RT-specimen and TR-specimen used in this study. Despite the use of different types of wood, the experimental results of this study have similar tendency with those of Aker et al. [4], indicating consistent behavior in combined perpendicular-to-grain normal and rolling shear strength behavior.

Since the strengths have discrepancy and also clustering, they are roughly categorized into three regions for the ease comparison of the applicability of different strength criteria. The stress combination zones

https://doi.org/10.52202/080513-0018

are able to cover the majority of data and guarantee that the same strength criteria cannot pass two different zones simultaneously at certain normal stress. The tensile shear strength zone is denoted by zone I, while the compressive-shear test data is divided into two parts: zone II and zone III , characterized by stress states $\left(\sigma_{c,I},\tau_J\right) \in \left\{f_{c,I} \le \sigma_{c,I} \le 0\ ,\ f_{v,J} \le \tau_J \le 1.6 f_{v,J}\right\}$ and $\left(\sigma_{c,I},\tau_J\right) \in \left\{1.3 f_{c,I} \le \sigma_{c,I} < 0.5 f_{c,I},\ 0 \le \tau_J < f_{v,J}\right\}$, respectively.

It is noteworthy that each strength criterion possesses different capabilities in describing the strength failure behavior of wood under combined normal-shear stress, and no single criterion can be applied simultaneously to all three stress zones. In the future, it is important to propose strength criteria that are continuous, smooth, and applicable across all three stress zones to support good constitutive model for nonlinear mechanical analysis of timber structures.

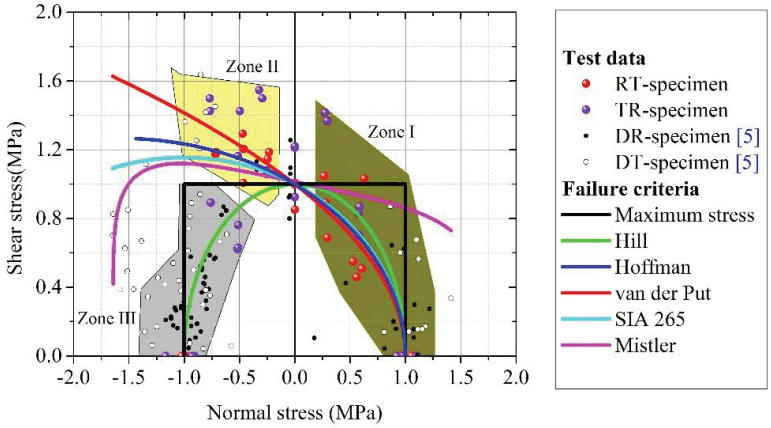

Figure 8. Comparison of commonly employed criteria for wood utilizing combined transverse tension/compression and rolling shear strength data.

4.3 LR AND LT SPECIMENS

Comparison of commonly employed criteria for wood utilizing combined transverse tension/compression and rolling shear strength data was shown in Figure 9.

The maximum stress criterion and Mistler criterion have poor performance in characterizing the strength of wood under biaxial stress, so the k values of both are no longer calculated. It can be seen that the prediction results of several strength criteria show higher accuracy in the first quadrant, that is, the prediction of the tensile shear stress part of wood is more accurate. In the first quadrant, the k values of Hill and Hasebe criteria are smaller compared to other criteria. Hill criterion uses compressive strength for strength prediction with higher accuracy for normal stress, while in the second quadrant, only Hasebe criterion has more accurate prediction results. In summary, the Hill criterion and Hasebe criterion have better representation effects in predicting the positive strength of wood.

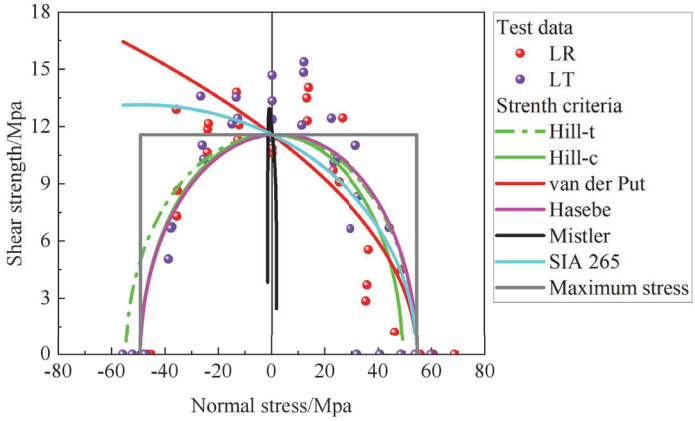

Figure 9. Comparison of commonly employed criteria for wood utilizing combined transverse tension/compression and rolling shear strength dat

6 – CONCLUSION

(1) The van der Put and SIA 265 criteria can be adopted to predict the longitudinal shear failure of wood under

https://doi.org/10.52202/080513-0018

different constraint levels of normal stress, and the least error was produced by the former.

(2) van der Put and Hill criteria were identified as the most suitable for describing specific aspects of wood strength under combined transverse normal and rolling shear stresses.

(3) The Hill and Hasebe criteria minimizes the error in predicting the longitudinal normal and transversal shear strength interaction behaviour.

7 – REFERENCES

[1] R. Spengler. “Festigkeitsverhalten von Brettschichtholz unter zweiachsiger Beanspruchung. Ermittlung des Festigkeits-verhaltens von Brettelementen aus Fichte durch Versuche.” Technische UniversitätMünchen, 1982.

[2] H. Mistler. “Die Tragfähigkeit des am Endauflager unten rechtwinklig ausgeklinkten Brettschichtträgers.” Lehrstuhl für Ingenieurholzbau und Baukonstruktionen, Technische Hochschule Karlsruhe, Germany, 1979.

[3] F. Keenan. “Shear strength of wood beams.” Forest Products Journal, 1974, 24(9): 63-70.

[4] Bilko P, Skoratko A, Rutkiewicz A, et al. Determination of the Shear Modulus of Pine Wood with the Arcan Test and Digital Image Correlation[J]. Materials, 2023, 14(2): 468.

[5] Akter ST, Bader TK. Experimental assessment of failure criteria for the interaction of normal stress perpendicular to the grain with rolling shear stress in Norway spruce clear wood[J]. European Journal of Wood and Wood Products, 2020, 78(6): 1105-1123.

https://doi.org/10.52202/080513-0018